Influence of deposition rate on magnetic properties of inverse-spinel NiCo2O4epitaxial thin films grown by pulsed laser deposition

AUTHOR(S):

Kan, Daisuke; Suzuki, Ikumi; Shimakawa, Yuichi

Influence of deposition rate on magnetic properties of inverse-spinel $NiCo_2O_4$ epitaxial thin films grown by pulsed laser deposition

Daisuke Kan[1,*], Ikumi Suzuki[1], and Yuichi Shimakawa[1]

[1]Institute for Chemical Research, Kyoto University, Uji, Kyoto 611-0011, Japan

electronic mail: [a)]dkan@scl.kyoto-u.ac.jp

We investigated the influence of the deposition rate on structural and magnetic properties of inverse-spinel ferrimagnet $NiCo_2O_4$ epitaxial films grown by pulsed laser deposition. While films' lattice constants are insensitive to the deposition rate, saturation magnetization and perpendicular magnetic anisotropy for the film grown with a high deposition rate are reduced. These results imply that growing $NiCo_2O_4$ films with a high deposition rate leads to occupations of the tetrahedral site by Ni, although Ni ideally occupies only the octahedral site. Controlling the deposition rate and modulating the cation distribution is key for tuning the magnetic properties in $NiCo_2O_4$ films.

A variety of magnetic and transport properties for ternary spinel oxides AB_2O_4 depend on cation occupation and distribution in crystallographically distinct tetrahedral (T_d) and octahedral (O_h) sites[1-7]. The inverse spinel $NiCo_2O_4$ (NCO)[8-12] in which the Co ideally occupies in both T_d and O_h sites and Ni occupies only the O_h site is a half-metallic ferrimagnet with a transition temperature above 400 K, attracting attention as a spintronic material[6,13-21]. It has been shown that when NCO films are epitaxially grown by pulsed laser deposition, depositing NCO under relatively high oxygen pressures like 100mTorr is a key for fabricating films having properties comparable to bulk[20,22,23] for example, a large saturation magnetization of ~2μ_B/f.u. and a high transition temperature above 400 K. Resonant x-ray diffraction measurements have recently shown that cation occupation in such high-quality NCO films still deviates from the stoichiometric occupation: about 15% Co in the T_d-site is replaced by Ni while Co and Ni almost equally occupy the O_h site[22]. It should also be pointed out that T_d-site cations play key roles in magnetizations and perpendicular magnetic anisotropy of NCO epitaxial films[20,24,25]. An important implication is that tuning growth conditions of NCO films and modifying the T_d-site cation occupation would control films' magnetic properties.

Given that the deposition rate (or growth rate) is closely associated with non-equilibrium film growth by physical vapor deposition techniques such as pulsed laser deposition, changing the deposition rate is expected to modify cation occupation and arrangement in grown films. In this study, we controlled the deposition rate during film growth by pulsed laser deposition and investigated structural, magnetic, and transport properties of NCO epitaxial films grown with distinct deposition rates.

Epitaxial films of NCO 30 nm thick were grown on (100) $MgAl_2O_4$ (MAO) substrates by pulsed laser deposition. During the film deposition, the substrate temperature and oxygen pressure were kept at 315°C and 100mTorr, respectively. A $NiCo_2O_x$ ceramic target was ablated at 6 Hz with a KrF excimer laser with a laser power of 130mJ. The deposition rate was controlled by changing the

width of a slit installed in front of a focusing lens equipped with a PLD chamber. Here we focus on two NCO films grown with high and low deposition rates in our setup (0.011nm/pulse and 0.0038nm/pulse, respectively) and discuss how the deposition rate affects structural, magnetic, and transport properties of NCO films. Hereafter these two films are referred to as the high-rate film and the low-rate film. We have previously shown that NCO films grown under the same conditions as those used for growing the low-rate film have a large room-temperature magnetization (~1 μ_B/f.u) and sufficient perpendicular magnetic anisotropy (~0.2 MJ/m^3 in the magnetic anisotropy energy at room temperature)[13,22].

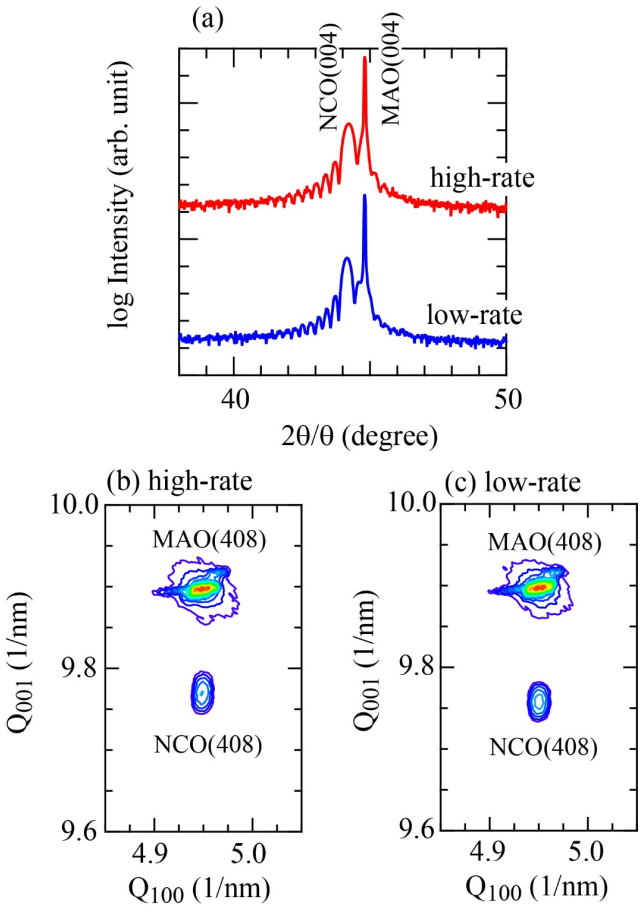

Figure 1: (a) X-ray 2θ/θ diffraction profiles for the high-rate film and the low-rate film. (b and c) Reciprocal space mappings around the (408) $MgAl_2O_4$ reflection for the high-rate film and the low-rate film.

Figure 1a shows x-ray 2θ/θ diffraction patterns around the (004) MAO reflection for the high-rate film and the low-rate film. Regardless of the deposition rate, these two films exhibit the (004) NCO reflections associated with clear thickness fringes, and there are no peaks from secondary phases observed. The out-of-plane lattice parameters of these two films are about the same, 8.19 Å for the high-rate film and 8.20 Å for the low-rate film. The reciprocal space mapping measurements around the (408) MAO reflection (Fig. 1b) show that the (408) reflections of both high-rate and low-rate films appear in the same position along the horizontal axis (the in-plane direction) as those for the substrates. This confirms that the NCO layers are coherently grown on the substrate and are under the substrate-induced compressive strain (~0.4%), regardless of the

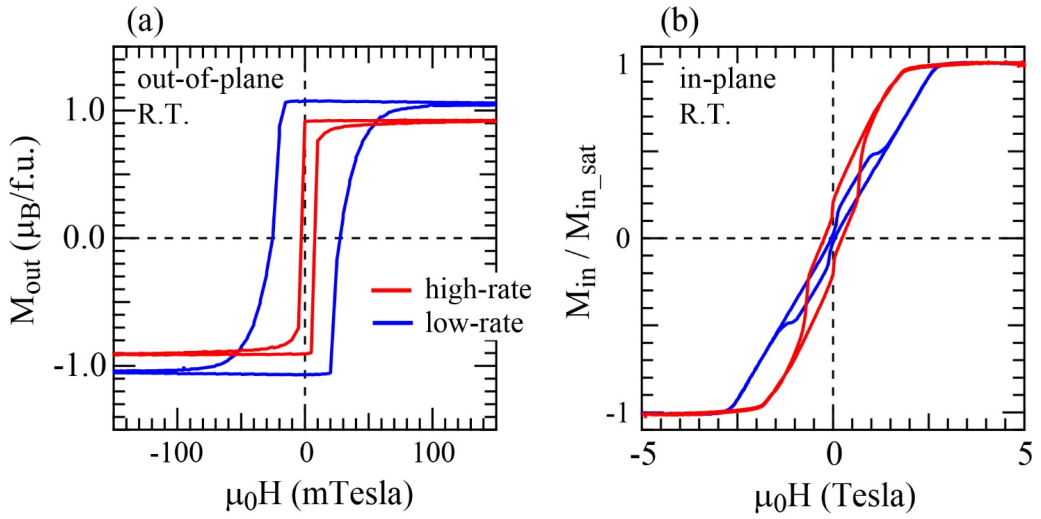

Figure 2: Room-temperature magnetic field dependence of the (a) out-of-plane and (b) in-plane magnetization for the high-rate film (red) and the low-rate film (blue). In (b), the magnetization is normalized by the magnetization value at 5 Tesla.

deposition rate.

In contrast to the insensitivity of the films' lattice constants to the deposition rate, the films' magnetic properties are found to depend on the deposition rate. Figure 2a shows the room-temperature magnetic field dependence of the out-of-plane magnetizations. For both films, the

out-of-plane magnetization exhibits square-shaped hysteresis loops against the field sweep directions, and the residual magnetizations are also comparable to the saturated one. The saturation magnetization (M_s) for the high-rate film, 0.92 μ_B/f.u. is slightly lower than that for the low-rate film, 1.05μ_B/f.u. The coercive fields H_c differ largely between these two films, and the H_c for the high-rate film is 5 mTesla, one-fifth of that for the low-rate film, 25 mTesla. These observations indicate that both films have out-of-plane magnetization, but the magnetic anisotropy varies depending on the deposition rate.

The influence of the deposition rate on the films' magnetic anisotropy is also inferred from the room-temperature magnetic field dependence of the in-plane magnetization shown in Figure 2b. The in-plane magnetization gradually increases with increasing the field strength and saturates in the large field region. A small hysteresis seen in the low magnetic field regions is probably due to misalignments of the films having relatively small Hc, although the origin of the hysteresis behavior has not been identified. We define the anisotropy field H_k as the minimum magnetic field necessary to saturate the in-plane magnetization. The H_k for the high-rate film and the low-rate film are 1.8 Tesla and 2.7 Tesla, respectively. The magnetic anisotropy energy (MAE) calculated by taking MAE = $M_s \cdot H_k/2$ is 0.11 MJ/m^3 for the high-rate film and 0.20 MJ/m^3 for the low-rate film, confirming that the high-rate film has a lower MAE than the low-rate film.

Figure 3 shows the temperature dependence of the M_s, the H_c, the H_k, and the electrical resistivity ρ_{xx} for the high-rate film and the low-rate film. The ρ_{xx} was measured by a van der Pauw method. The temperature dependence of the M_s for the high-rate film and the low-rate film follow the same trend, and the M_s for the high-rate film is slightly lower than that of the low-rate film in the entire temperature range. These observations indicate that the high-rate film has a slightly lower transition temperature than the low-rate film. In addition, as shown in Figures 3b and 3c, both H_c and H_k for the high-rate film are lower than those for the low-rate film in the entire temperature range,

confirming the lowering of the MAE for the high-rate film.

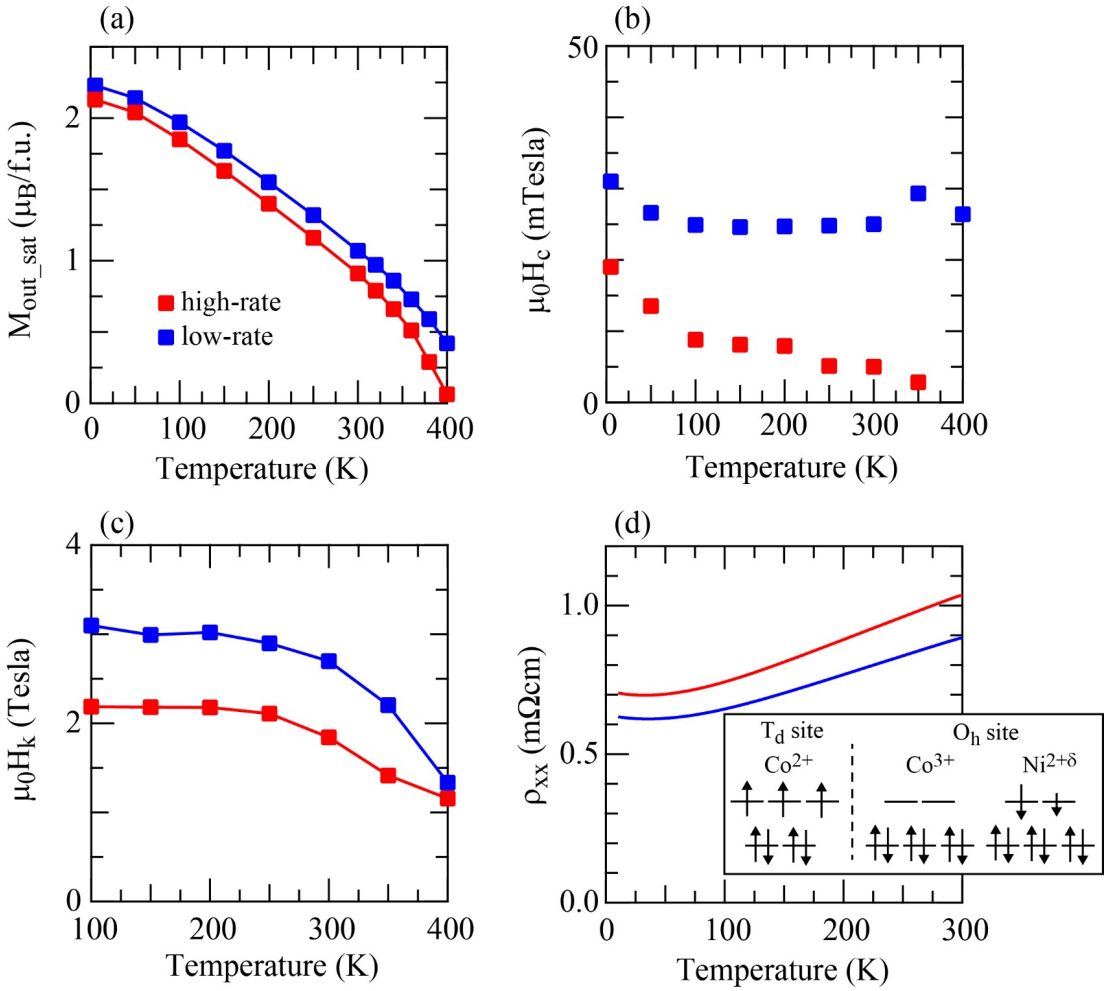

Figure 3: Temperature dependence of the (a) the out-of-plane saturation magnetization M_s, (b) coercive field H_c, (c) anisotropy field H_k, and (d) electrical resistivity ρ_{xx} for the high-rate film (red) and the low-rate film (blue). The magnetizations in (a) were extracted from the magnetic field dependence of the out-of-plane magnetization measured at temperatures between 5 K and 400 K. In the inset of (d), spin configurations of $NiCo_2O_4$ are presented. The configurations are drawn by assuming that the valence states of the T_d-site Co, the O_h-site Co and the O_h-site Ni are +2, +3 and +(2+δ), respectively. The short arrow for $Ni^{(2+\delta)+}$ represents partial (δ) occupation of the orbital. For T_d-site Co, the upper three states consist of d_{xy} d_{xz}, and d_{yz} orbitals. For the O_h-site cations, the lower three states consist of d_{xy} d_{xz}, and d_{yz} orbitals.

We now consider the origin of the deposition-rate-dependent changes in the magnetic

properties of NCO films. The concentration of oxygen vacancies (or oxygen defects) might differ between the high-rate film and the low-rate film. It has been shown that introducing oxygen vacancies into $NiCo_2O_4$ leads to a slight reduction in the saturation magnetization, but its influence on the H_k is negligibly small[26]. Thus oxygen vacancies (or the oxygen concentrations) are not a prime cause for the deposition-rate-dependence of the magnetic properties of NCO films. We also note that lowering the Ni occupation (or increasing the Co occupation) in the O_h-site of NCO films causes reductions in the saturation magnetization and the transition temperature[22]. For such films with the low Ni occupation in the O_h-site (referred to as the low-Ni film), the H_c is much larger than those for the high-rate film and the low-rate film investigated in this study, and the H_k increases with decreasing temperature and reaches ~5 Tesla at 100 K (see Supplementary Information Figure S1). These behaviors in H_c and H_k for the low-Ni films totally differ from the deposition-rate-induced changes in magnetic properties of NCO films. Therefore, depositing NCO with the high growth rate probably does not result in the lowering of the Ni occupation in the O_h-site of the films. It should be pointed out that the perpendicular magnetic anisotropy in NCO films is predominantly determined by the out-of-plane orbital magnetic moment originating from the T_d-site Co[24,25]. The observed reduction in the MAE for the high-rate film implies that the magnitude of the orbital magnetic moment from the T_d-site cations is reduced when NCO films are deposited with the high growth rate. Previous x-ray absorption spectroscopy indicated that in the NCO films grown under 100mTorr oxygen pressure (corresponding to the low-rate film in this study), the Co in the T_d- and O_h-site have a valence state close to +3 and +2 while the valence state of the O_h-site Ni is close to +2.5[24]. Given the nominal number of *d* electrons in Co^{2+} (d^7), Co^{3+} (d^6), and $Ni^{2.5+}$ ($d^{7.5}$) and spin configurations of these cations (the inset of Figure 3d), replacing the T_d-site Co by Ni probably reduces not only the magnetization but also the magnitude of the orbital moment from the T_d-site sublattice. It is thus reasonable to consider that depositing NCO with the high rate leads to Ni occupation in the T_d site,

modulating the cation distribution in NCO films and influencing the films' magnetic properties. In addition, the modification in the T_d-site cation occupation should concomitantly change the O_h-site cation occupation, causing a slight increase in the Co occupation (decrease in the Ni occupation) of the O_h site. Because the density of states at the Fermi level in NCO consists of spin-down e_g electrons of the O_h-site Ni[6,16,27], the deposition-rate-induced decrease in the O_h-site Ni occupation should reduce electrical conductions. Figure 3d shows the temperature dependence of the ρ_{xx} for the high-rate film and the low-rate film. While both films exhibit metallic transport behavior, the ρ_{xx} for the high-rate film is slightly higher than that for the low-rate film, which is in agreement with our scenario that depositing NCO at the high rate leads to Ni occupations of the T_d site.

In summary, we investigate how the deposition rate influences structural, magnetic, and transport properties of the inverse spinel $NiCo_2O_4$ epitaxial thin films. We found that the lattice constants of the films are almost independent of the deposition rate. In contrast, both total magnetization and the perpendicular magnetic anisotropy are reduced for the film grown with the high deposition rate. These behaviors can be understood by taking into consideration that growing $NiCo_2O_4$ films at the high deposition rate leads to Ni occupation into the T_d site although Ni ideally occupies only the O_h site. These results indicate that controlling the deposition rate and modulating the cation distribution is a key for tuning the magnetic properties of $NiCo_2O_4$ films.

This work was partially supported by a grant for the Integrated Research Consortium on Chemical Sciences, by Grants-in-Aid for Scientific Research (Grant Nos. JP16H02266, JP17H04813, JP19H05816, and JP19H05823), by a JSPS Core-to-Core program (A), by a grant for the Joint Project of Chemical Synthesis Core Research Institutions from the Ministry of Education, Culture, Sports, Science and Technology (MEXT) of Japan, and by ISHIZUE 2020 of Kyoto University Research Development Program.

Data Availability Statement

The data that support the findings of this study are available from the corresponding author upon reasonable request.

References

1 J. D. Dunitz and L. E. Orgel, J. Phys. Chem. Solids **3** 318 (1957).

2 X. Batlle, X. Obradors, J. Rodríguez‐Carvajal, M. Pernet, M. V. Cabañas, and M. Vallet, J. Appl. Phys. **70** 1614 (1991).

3 E. J. W. Verwey, F. d. Boer, and J. H. v. Santen, The Journal of Chemical Physics **16** 1091 (1948).

4 A. Zakutayev, T. R. Paudel, P. F. Ndione, J. D. Perkins, S. Lany, A. Zunger, and D. S. Ginley, Phys. Rev. B **85** 085204 (2012).

5 T. R. Paudel, A. Zakutayev, S. Lany, M. d'Avezac, and A. Zunger, Adv. Funct. Mater. **21** 4493 (2011).

6 P. F. Ndione, Y. Shi, V. Stevanovic, S. Lany, A. Zakutayev, P. A. Parilla, J. D. Perkins, J. J. Berry, D. S. Ginley, and M. F. Toney, Adv. Funct. Mater. **24** 610 (2014).

7 D. Das and S. Ghosh, J. Phys.: Condens. Matter **29** 055805 (2016).

8 J. F. Marco, J. R. Gancedo, M. Gracia, J. L. Gautier, E. Ríos, and F. J. Berry, J. Solid State Chem. **153** 74 (2000).

9 D. Pyke, K. K. Mallick, R. Reynolds, and A. K. Bhattacharya, J. Mater. Chem. **8** 1095 (1998).

10 O. Knop, K. I. G. Reid, Sutarno, and Y. Nakagawa, Can. J. Chem. **46** 3463 (1968).

[11] P. D. Battle, A. K. Cheetham, and J. B. Goodenough, Mater. Res. Bull. **14** 1013 (1979).

[12] J. F. Marco, J. R. Gancedo, M. Gracia, J. L. Gautier, E. I. Ríos, H. M. Palmer, C. Greaves, and F. J. Berry, J. Mater. Chem. **11** 3087 (2001).

[13] Y. Shen, D. Kan, I.-C. Lin, M.-W. Chu, I. Suzuki, and Y. Shimakawa, Appl. Phys. Lett. **117** 042408 (2020).

[14] K. Zhang, C. Zhen, W. Wei, W. Guo, G. Tang, L. Ma, D. Hou, and X. Wu, RSC Advances **7** 36026 (2017).

[15] C. Zhen, X. Zhang, W. Wei, W. Guo, A. Pant, X. Xu, J. Shen, L. Ma, and D. Hou, J. Phys. D: Appl. Phys. **51** 145308 (2018).

[16] M. Wang, X. Sui, Y. Wang, Y.-H. Juan, Y. Lyu, H. Peng, T. Huang, S. Shen, C. Guo, J. Zhang, Z. Li, H.-B. Li, N. Lu, A. T. N'Diaye, E. Arenholz, S. Zhou, Q. He, Y.-H. Chu, W. Duan, and P. Yu, Adv. Mater. **31** 1900458 (2019).

[17] X. Chen, X. Zhang, M.-G. Han, L. Zhang, Y. Zhu, X. Xu, and X. Hong, Adv. Mater. **31** 1805260 (2019).

[18] P. Silwal, L. Miao, J. Hu, L. Spinu, D. H. Kim, and D. Talbayev, J. Appl. Phys. **114** 103704 (2013).

[19] P. Pandey, Y. Bitla, M. Zschornak, M. Wang, C. Xu, J. Grenzer, D.-C. Meyer, Y.-Y. Chin, H.-J. Lin, C.-T. Chen, S. Gemming, M. Helm, Y.-H. Chu, and S. Zhou, APL Materials **6** 066109 (2018).

[20] Y. Bitla, Y.-Y. Chin, J.-C. Lin, C. N. Van, R. Liu, Y. Zhu, H.-J. Liu, Q. Zhan, H.-J. Lin, C.-T. Chen, Y.-H. Chu, and Q. He, Scientific reports **5** 15201 (2015).

[21] A. Tsujie, Y. Hara, T. Yanase, T. Shimada, and T. Nagahama, Appl. Phys. Lett. **116** 232404 (2020).

[22] Y. Shen, D. Kan, Z. Tan, Y. Wakabayashi, and Y. Shimakawa, Phys. Rev. B **101** 094412 (2020).

[23] C. Wu, W. Guo, C. Zhen, H. Wang, G. Li, L. Ma, and D. Hou, J. Appl. Phys. **126** 043901 (2019).

[24] D. Kan, M. Mizumaki, M. Kitamura, Y. Kotani, Y. Shen, I. Suzuki, K. Horiba, and Y. Shimakawa, Phys. Rev. B **101** 224434 (2020).

[25] C. Mellinger, J. Waybright, X. Zhang, C. Schmidt, and X. Xu, Phys. Rev. B **101** 014413 (2020).

[26] I. Suzuki, D. Kan, M. Kitamura, Y. Shen, K. Horiba, and Y. Shimakawa, J. Appl. Phys. **127** 203903 (2020).

[27] R. Zhang, M. Liu, W. Liu, and H. Wang, Mater. Lett. **199** 164 (2017).